Microsc. Microanal. Microstruct. **8** (1997) 103–113 APRIL **1997**, PAGE 103

Atomic Scale Imaging and Analysis of T′ Precipitates in Al-Mg-Zn Alloys

Annabelle Bigot ([1]), Pierre Auger ([1]), Sylvain Chambreland ([1]), Didier Blavette ([1]) and Andrew Reeves ([2])

([1]) Équipe Sonde Atomique et Microstructures, Groupe de Métallurgie Physique, UMR CNRS 6634, Faculté des Sciences, Place Émile Blondel, 76821 Mont Saint Aignan Cedex, France
([2]) Pechiney Centre de Recherches de Voreppe, BP 27, 38340 Voreppe, France

(Received September 25, 1996; accepted February 14, 1997)

PACS.07.81.+a – Electron, ion spectrometers, and related techniques
PACS.68.35.-p – Solid surfaces and solid-solid interfaces
PACS.81.30.Mh – Solid-phase precipitation

Abstract. — The composition, morphology and volume fraction of the metastable T′ phase formed in an industrial Al-4.91wt%Mg-3.20wt%Zn alloy have been investigated using the tomographic atom probe. Roughly globular and sometimes elongated T′ precipitates are present in the alloy aged at 140 °C for 24 hours after solution heat treatment and water quenching, with a number density of 1.8×10^{17} cm^{-3}. The volume fraction of the phase is close to 4.5%. The T′ precipitates were found to have an average composition of 37.5 at% Mg, 36.5 at% Al and 26 at% Zn, which is, within experimental error, identical to that of the stable T phase $Mg_{32}(Al, Zn)_{49}$.

Résumé. — La composition, la morphologie et la fraction volumique de la phase métastable T′ formée par revenu d'un alliage industriel Al-4,91wt%Mg-3,20wt%Zn (24 heures à 140 °C après mise en solution et trempe) ont été déterminées en sonde atomique tomographique. Les précipités T′, de forme généralement globulaire et parfois allongée, sont rencontrés avec une densité numérique de $1{,}8 \times 10^{17}$ cm^{-3}. La fraction volumique de la phase est proche de 4,5 %. La composition moyenne des précipités T′ analysés est de 37,5 %at Mg, 36,5 %at Al et 26 %at Zn, ce qui correspond, aux incertitudes près, à la stoechiométrie $Mg_{32}(Al, Zn)_{49}$ de la phase stable T.

1. Introduction

Al-Zn-Mg-(Cu) alloys (7XXX series) are of great industrial interest thanks to their capability to undergo age hardening and thus reach very high mechanical strengths. The hardening process takes place during ageing at low temperatures, after solution treatment and quench, and results from microstructural changes in the alloy, namely the formation of GP zones and the precipitation of metastable phases.

The detailed knowledge of the microstructural features of Al-Zn-Mg-(Cu) alloys after ageing is required for the improvement of their mechanical performances. For this reason, the size,

Table I. — *Nominal alloy composition, in atomic and weight percentages.*

	Al	Mg	Zn	Mn	Zr
at%	92.97	5.54	1.34	0.12	0.03
wt%	91.55	4.91	3.20	0.23	0.11

morphology and crystallography of hardening phases have been extensively studied. The decomposition sequence of the aluminium supersaturated solid solution, as determined by numerous works in the past years, can be summarized as follows:

$$\begin{aligned} \text{ss} &\rightarrow \text{GP zones} \rightarrow \eta'(\text{metastable}) \rightarrow \eta \\ \text{ss} &\rightarrow \text{T}'(\text{metastable}) \rightarrow \text{T}. \end{aligned}$$

However, little information is available on the composition of both the solid solution and the precipitates formed during ageing.

Atom probe (AP) techniques have been used to clarify this aspect of the precipitation hardening in 7XXX series alloys. Thanks to their ultra-high spatial resolution, atom probes are powerful analysis instruments that are well suited to the investigation of the early stages of phase transformations in alloys. The tomographic atom probe (TAP) is a new generation of AP which provides 3-dimensional images of the analysed material. As a result of this 3D vision, the morphology and composition of individual precipitates can be determined. Results about GP zones formed at room temperature in AA 7150 have been already published [1]. The study of η' and η phases in the same alloy has been reported elsewhere [2].

The present paper focuses on the T′ phase, which is formed during low temperature ageing of alloys with moderate to high Mg/Zn ratios. These alloys lie in the (alpha + T) equilibrium phase field of the diagram at 200 °C [3].

The structure of the T phase is based on a body centered cubic lattice with $a = 1.416$ nm [4]. The unit cell contains 162 atoms. Whereas the atomic percentage of magnesium is thought to be nearly constant, the Al/Zn ratio can vary. The occupancy of the Al and Zn sites is disordered and probably only partial for some of the sites [4, 5], which justifies the general formula $Mg_{32}(Al, Zn)_{49}$. The T′ phase has also a bcc crystal structure with a lattice parameter close to that of the T phase: $a = 1.44$ to 1.45 nm [6]. Slightly different parameters were reported more recently: $a = 1.435$ nm for T′ and $a = 1.461$ nm for T [7]. The orientation relationships between matrix and precipitates are the same for the T′ and T phases [6, 7]: $(100)_{T'} \parallel (111)_{Al}$ and $(010)_{T'} \parallel (11\bar{2})_{Al}$.

Most aluminium alloys follow a multi stage decomposition sequence including the formation of metastable phases. Therefore, the T phase has been naturally supposed not to form directly from the solid solution during ageing at temperatures between 120 and 200 °C. Moreover, the small size and low volume fraction of precipitates make the identification of the phase difficult with conventional techniques, and the precipitates observed have been called T′. However, considering the similarity of crystal lattice and epitaxy relations of the two phases, the question arises if T′ and T are not the same phase. In fact, the only reason to distinguish between them would be their composition.

2. Experimental

2.1. Alloy Composition and Heat Treatment

The nominal composition of the alloy sample supplied by Pechiney Rhénalu is given in Table I. The choice of an alloy with a high Mg to Zn ratio simplifies the identification of the present

phases by TEM as a high number density of T′ precipitates can be obtained. The small Zr and Mn additions lead to the formation of Zr and Mn rich dispersoids, which reduces recrystallization and grain growth.

The sample, in the form of a bar 8×8 mm^2 in section, was solution treated at 478 °C for 2 hours, water quenched and introduced in the hot furnace to be aged at 140 °C for 24 hours. After this ageing time, the alloy is in the peak strength condition (T6 temper). T′ precipitates formed during ageing are responsible for the hardening.

2.2. Transmission Electron Microscopy

Thin foils were prepared by twin-jet electropolishing using a 30% perchloric acid-methanol solution at $-35/-40$ °C with a DC voltage of 20 V. Observations were performed in a 120 kV Zeiss Omega 912 transmission electron microscope. Elastic bright-field/dark-field images and selected area diffraction patterns were obtained using the Zeiss Omega filter [8].

2.3. The Tomographic Atom Probe Technique

The TAP designed at Rouen University was used for composition analyses. The basis of AP instruments is the field evaporation of ions from the surface of a very sharp-tipped sample. The ions of different chemical species are received by a detector and identified by time of flight mass spectrometry. The TAP is equipped with a multi-event position sensitive detector. The positions of ion impacts on the detector are recorded so that the analysed material can be 3D reconstructed. After the analysis, any part of the reconstructed volume can be investigated in order to measure local composition of solid solution and precipitates. The tomographic atom probe is a projection microscope, thus the size of the analysis area is determined by the dimensions of the detector (8×8 cm^2) and the radius of curvature of the sample (≈ 50 nm). A few hundred thousand atoms are collected during an analysis and the reconstructed volume is typically $15 \times 15 \times 50$ nm^3. Further details about this instrument are reported elsewhere [9].

Tip samples were electropolished in a solution of HNO_3 (1/3) and methanol (2/3) cooled to below -10 °C at a DC voltage of 5 to 8 V. Analyses were carried out under the following conditions: tip temperature 20 to 40 K, pulse to standing voltage 20%, vacuum better than 10^{-8} Pa.

The three-dimensional reconstruction of the analysed material, and therefore the depth calibration of the 3D images obtained, require the knowledge of space parameters, related to the evaporation field of the material and the position of the projection point [10]. These parameters were determined from ion micrographs. The depth calibration was then checked for different directions of analysis $[hkl]$. In every case, the lattice spacing of the reconstructed (hkl) planes has the correct value. This is an absolute criterion which confirms that the depth calibration is reliable.

A TAP mass spectrum of the Al-Zn-Mg alloy is shown in Figure 1. Magnesium and manganese atoms evaporate doubly charged only, whereas zinc and aluminium ions have both 2+ and 1+ states of charge. Some of the latter are also detected as AlH^+, AlH_2^+ and AlH_3^+ hydrides. The mass resolution at half maximum of peaks is close to $M/\Delta M = 100$. In these conditions, the very small Mn^{2+} peak (27.5 amu) cannot be extracted from the high level Al^+ (27 amu) peak, therefore the manganese concentration is included in the aluminium concentration data.

Local compositions are determined by counting the number of atoms of the different chemical species present in a small selected volume of the analysed and 3D reconstructed material. The statistical standard deviation on a concentration C is $\sigma = \sqrt{C(1-C)/N}$, with N the number of atoms in the volume. In the following, compositions will be given within 2σ.

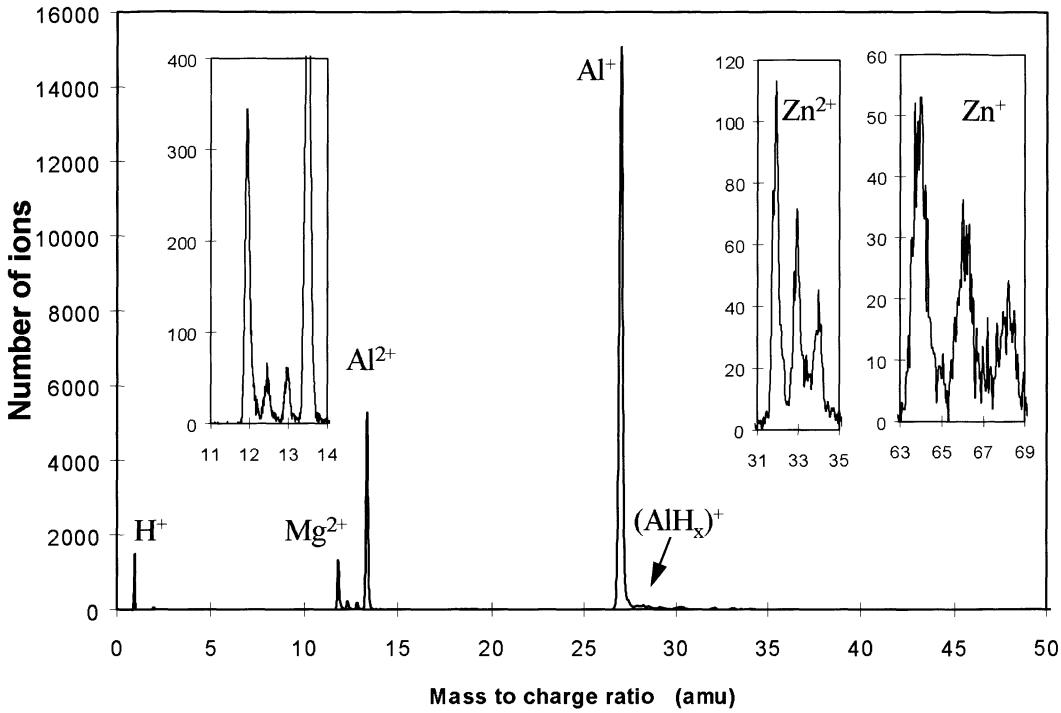

Fig. 1. — Tomographic atom probe mass spectrum of the Al-Mg 5.5-Zn 1.3 (at%) alloy.

Concentration profiles through a precipitate are obtained by counting the number of Al, Zn and Mg atoms present in a sampling volume moved step by step throughout the particle. This sampling volume is a flat box with lateral dimensions smaller than those of the precipitate in order to avoid contribution from the matrix.

3. Results and Discussion

3.1. Characterization of the Precipitation by TEM

The microstructure of the alloy aged for 24 hours at 140 °C is illustrated in Figure 2. The elastic bright-field images 2a and 2b show a dense population of essentially globular particles with diameters ranging from 5 to 20 nm. A comparison of the corresponding experimental 2c and calculated 2d $[112]_{Al}$ zone axis diffraction patterns confirms that a large majority of these precipitates have the crystal lattice, cell parameter and orientation relationships with the matrix that are common to both the T′ and T phases. An $(0\overline{3}\overline{5})_{T'}$ elastic dark-field image of T′ precipitates is shown Figure 2e. There is no Al_3Zr dispersoids in the investigated field.

3.2. Composition of the Residual Solid Solution

The solute concentrations in the solid solution of the aged alloy are 4.00 ± 0.18 at% Mg and 0.29 ± 0.05 at% Zn. The solid solution is much depleted in zinc whereas the relative variation of the Mg content remains moderate. The fact that precipitates have drained most of zinc atoms from the solid solution is particularly striking in Figure 3, which represents the distribution of Mg and Zn atoms in the aged Al-Mg 5.55-Zn 1.35 (at%) alloy analysed by TAP.

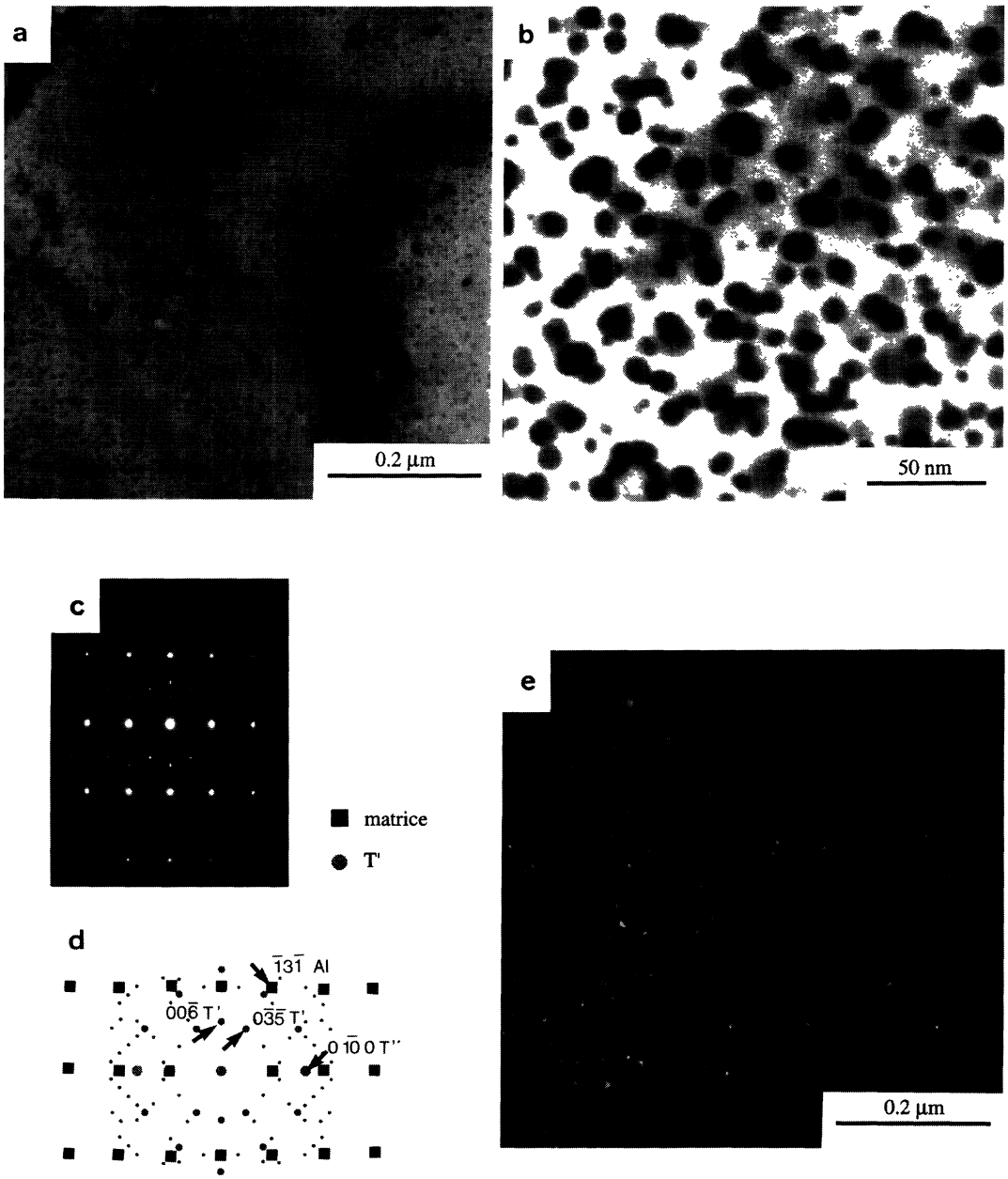

Fig. 2. — Elastic TEM bright field images (a, b) showing precipitates in the Al-Mg 5.5-Zn 1.3 (at%) alloy aged for 24 hours at 140 °C. The corresponding $[112]_{Al}$ zone axis diffraction pattern (c) is compared with a calculated pattern (d). The $(0\bar{3}\bar{5})_{T'}$ spot has been used to produce a dark-field image (e) of the T′ precipitates. The calculated diffraction pattern has not been corrected for the effects of double diffraction, which appear on the experimental pattern.

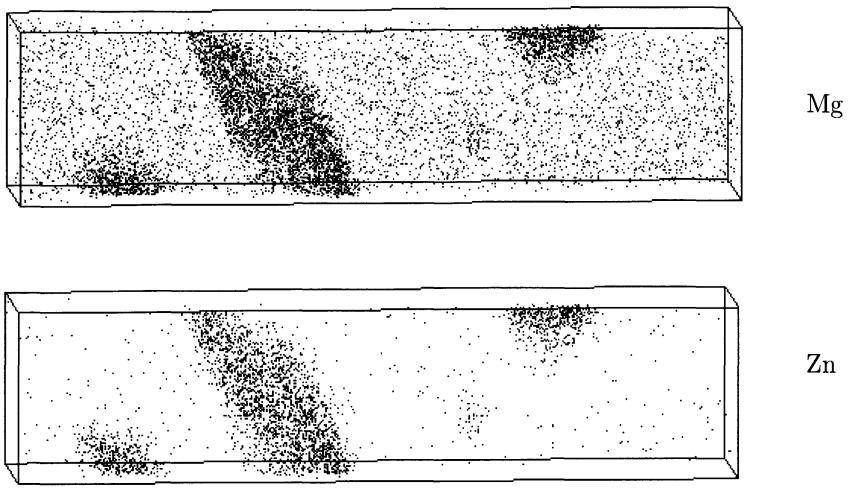

Fig. 3. — Elemental maps of Mg and Zn in a 3D reconstructed volume ($13 \times 13 \times 50$ nm^3) containing precipitates. Each point represents an atom.

Table II. — *Alloy composition, in atomic and weight percentages, determined from the whole analysis data collected.*

	Al (+Mn)	Mg	Zn	Zr
at%	93.9	4.85	1.25	0
wt%	92.7	4.3	3.0	0

3.3. Size, Morphology and Number Density of Precipitates

10 precipitates were analysed and 3D reconstructed. They seem to be regularly dispersed in the matrix. The total volume of material explored in the analyses performed is 65 000 nm^3. The number density of precipitates, estimated by counting the intercepted particles, is 1.8×10^{17} cm^{-3}. However, sampling randomly a material containing a low number density of particles by a relatively small volume leads to uncertainties. In the present case, the number density of precipitates may be slightly underestimated. This is confirmed by the measured alloy composition in Table II: The overall solute concentrations that are measured are somewhat lower than those expected (see Tab. I).

The shapes of reconstructed particles are clearly visualized by drawing surfaces of equal concentration in solute elements (shaded surfaces in Fig. 4). These isosurfaces correspond approximately to the precipitate-matrix interface. This kind of representation is obtained by further processing of the raw data illustrated in Figure 3.

Figure 4 shows typical morphologies of reconstructed particles. Most precipitates appear to be elongated globules with flattened or (less frequently) almost circular section, generally 3 to 5 nm in their small dimensions and 7 and to more than 10 nm in length. One of them is much bigger, 9×5 nm^2 in section and 20 nm long. Roughly equiaxed precipitates, sometimes slightly flattened, with dimensions ranging from 3 to 6 nm are also observed.

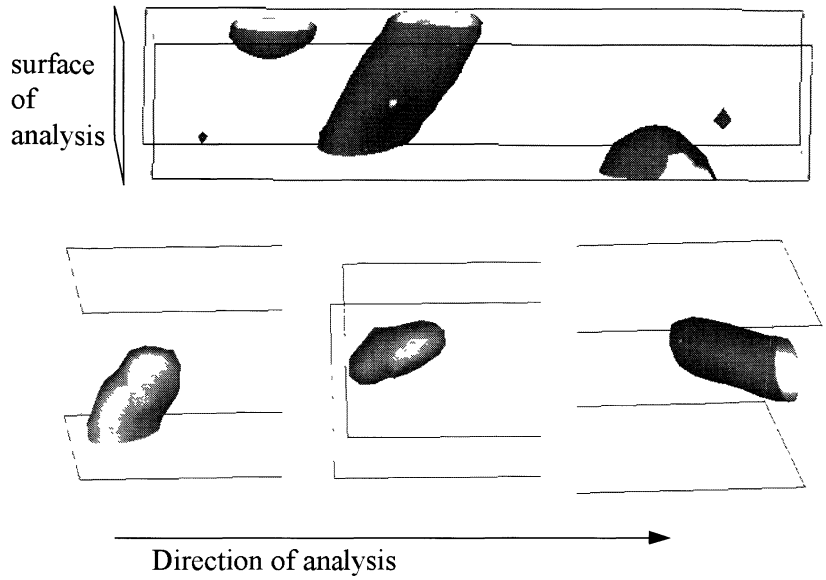

Fig. 4. — 3D reconstruction of precipitates in several analysed volumes. Surfaces of equal solute concentrations (in grey) show the precipitate shapes. Underestimation of the particle dimensions may occur in directions parallel to the analysis surface, resulting from magnification differences between the solid solution and precipitates.

These sizes and morphologies have to be considered carefully. The reconstruction of precipitates does not perfectly reflect their real aspect: in fact, the precipitates and the solid solution require different electric field strengths to evaporate. They develop different radii of curvature at the tip surface and are thus subject to local variations in magnification. The reconstruction process is global and based on the magnification of the solid solution, which is higher than that of the precipitate. This results in some possible underestimation of the lateral dimensions of precipitates and may account for their slightly smaller sizes than those determined by TEM. Their general morphology may also be deformed. Yet, if the local magnification effect was entirely responsible for the non equiaxed shapes, all particles would have their larger dimension along the direction of analysis. This is not observed, as demonstrated by Figure 4 which shows that some elongated particles were obtained whose long axis is inclined or almost perpendicular to the analysis direction. On the contrary, the flattened morphologies may be ascribed to the local magnification effect as the smallest dimension of precipitates is always parallel to the analysis surface.

Although the shapes of the reconstructed particles are not fully reliable, they strongly suggest the presence of elongated T′ precipitates in the alloy.

3.4. Composition of the Precipitated Phase, Nature of the Matrix-Precipitate Interface

The concentration profiles of Al, Mg and Zn across a T′ precipitate are presented in Figures 5a to 5c. The direction corresponding to the depth axis of the profiles is different from the direction of analysis, as shown in Figure 6. The direction of the concentration profiles is actually chosen so as to minimize precipitate and matrix convolution at the interface.

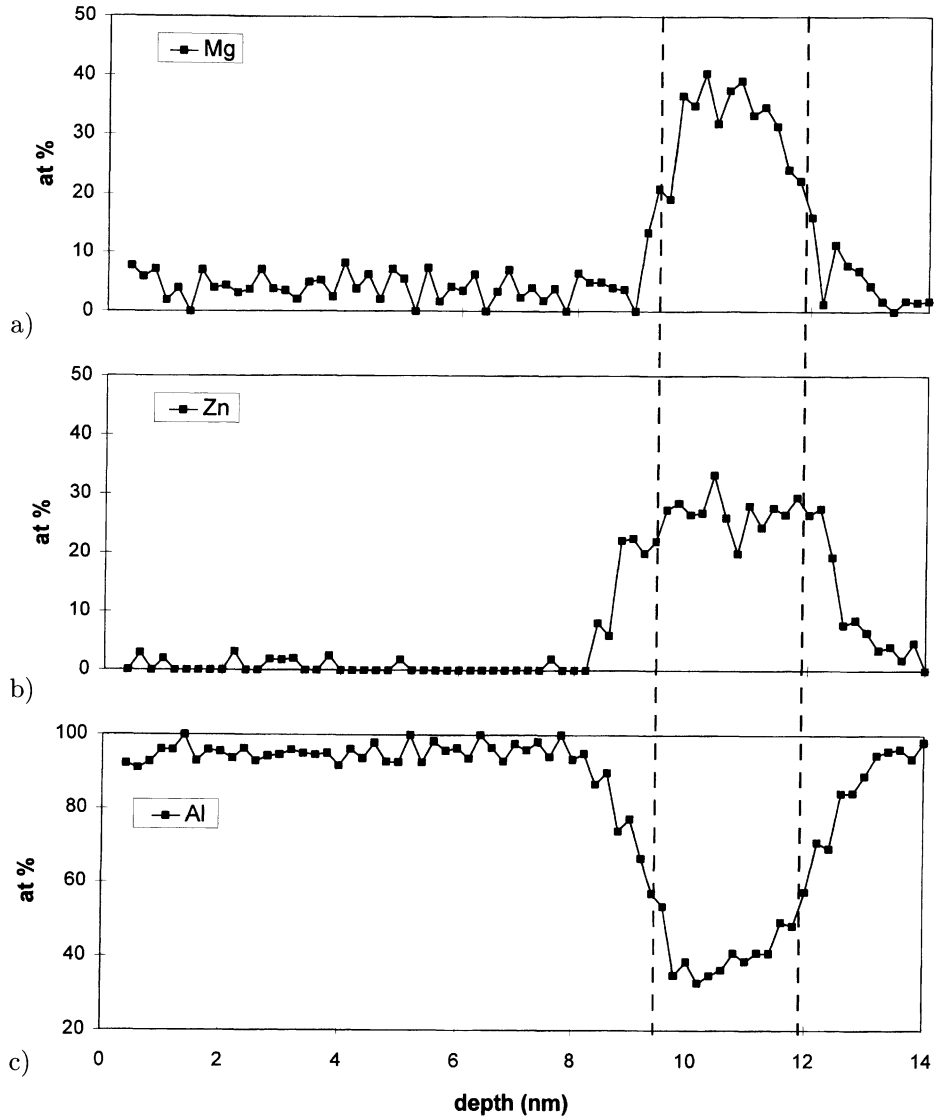

Fig. 5. — Concentration profiles of Mg (a), Zn (b) and Al (c) through a T′ precipitate. The composition is determined for each position of the sampling volume ($0.2 \times 3 \times 4$ nm^3).

A plateau is observed in the profiles, which confirms that the composition of the precipitate itself is measured. The transition region between the solid solution and the heart of the T′ particle partly results from sampling a round object with a parallelepiped. A feature is commonly observed in the concentration profiles of most T′ precipitates: the Zn concentration plateau is wider than the Mg concentration plateau, so the definition of the interface between T′ particle and matrix is not the same for the two solutes. The precipitates appear to be composed of a large Mg and Zn rich core surrounded by an outside layer poorer in magnesium. This suggests some non-equilibrium phenomenon, such as strain, which modifies the composition of the precipitate surface.

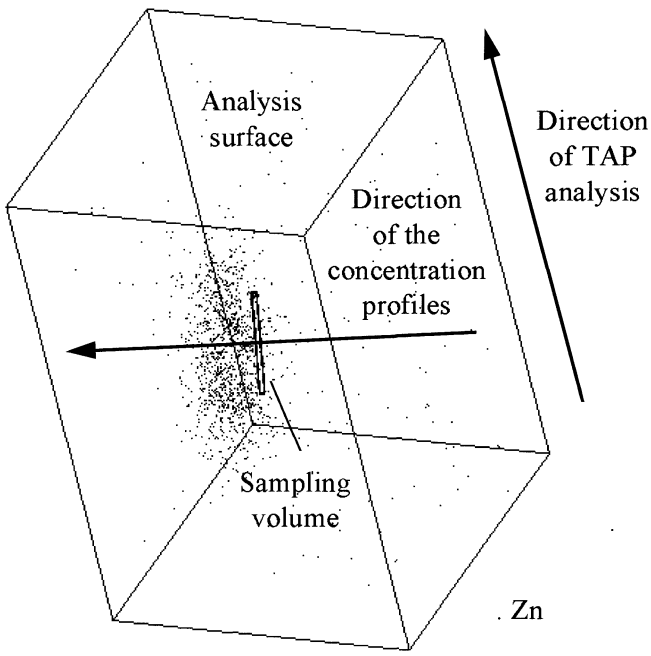

Fig. 6. — TAP analysed and 3D reconstructed volume of material ($13 \times 13 \times 20$ nm^3) containing the T′ particle which concentration profiles are displayed in Figure 5. Only zinc atoms are represented. The orientation of the sampling volume ($0.2 \times 3 \times 4$ nm^3) with respect to the direction of analysis and analysis surface is represented. The sampling volume is parallel to the precipitate/matrix interface.

Because of local magnification effects, caution must be taken in the interpretation of the solute levels at interfaces. However, the composition of the precipitate core is determined from the plateau part common to the Zn and Mg profiles. The data related to the 10 precipitates analysed are gathered in Table III and illustrated in Figure 7.

The statistical dispersion around the mean composition of the population is narrow. The Mg to (Al + Zn) ratio seems to be independent of the precipitate size. All precipitates are considered to belong to the T′ or T phase, as identified by TEM on structural and orientation criteria. The composition in the heart of precipitates roughly respects the general formula $Mg_{32}(Al, Zn)_{49}$ ascribed to the T phase. It contains less zinc than aluminium, which is not surprising if one considers the low nominal zinc concentration in the alloy.

3.5. Volume Fraction of T′ Phase

The concentrations of an element E in precipitates and matrix are related to the nominal composition of this element by the equation

$$C_{\mathrm{E}}^{\mathrm{nominal}} = xC_{\mathrm{E}}^{\mathrm{precipitate}} + (1-x)C_{\mathrm{E}}^{\mathrm{matrix}}, \tag{1}$$

where x is the precipitated atomic fraction. As the atomic volumes are very similar in the aluminium solid solution and in the $Mg_{32}(Al, Zn)_{49}$ structure (0.0165 nm^3 and 0.0175 nm^3 respectively), x is a close estimation of the volume fraction f_{v} of T′ precipitates.

The volume fraction $f_{\mathrm{v}} \approx x$ was calculated from equation (1) with E = Mg, Al, Zn, taking 37.5 at% Mg, 36.5 at% Al and 26 at% Zn as the composition of the phase. The f_{v} values

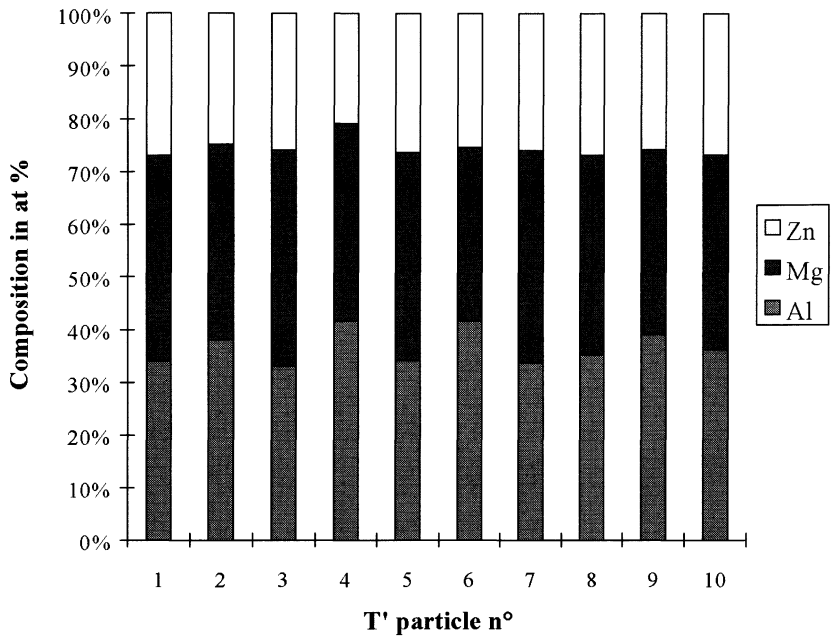

Fig. 7. — Compositions of the 10 precipitates analysed in Al-Mg 5.5-Zn 1.3 (at%) alloy annealed for 24 hours at 140 °C.

Table III. — *Composition of the precipitates, determined from concentration profiles. The size of particles is also indicated. The bottom lines of the table show the mean composition and the statistical dispersion of the population.*

n°	at% Mg	at% Al	at% Zn	size (nm × nm × nm)
1	39±3.5	34±3.5	27±3.5	3 × 3 × (> 4)
2	37±7	38±7	25±7	4 × 4 × (> 10)
3	41±4	33±4	26±3.5	3 × (> 3) × 10
4	37.5±3	41.5±3	21±2.5	(> 3) × 7 × (> 2)
5	39.5±3	34±3	26.5±3	4 × (> 4) × 7
6	33±3.5	41.5±4	25.5±3.5	(> 3) × (> 4) × (> 10)
7	40±3.5	33.5±3.5	26±3	(> 3) × 7 × (> 2)
8	38±3.5	35±3.5	27±3	5 × 9 × (> 17)
9	35±3	39±3.5	26±3	3 × 6 × 9
10	37±3	36±3	27±3	3 × 5 × 7
Mean	**37.7**	**36.6**	**25.7**	
σ	2.3	3.1	1.7	

corresponding to the different elements are coherent and close to 4.5% (Tab. IV). This volume fraction and the number density estimated before yield a mean diameter of precipitates $\emptyset = 7.8$ nm, in good agreement with the mean particle size observed.

Table IV. — *Volume fraction of T′ precipitates, calculated from (1) with the nominal composition Al-5.55 Mg-1.35 Zn (at%).*

volume fraction	E = Mg in Eq. (1)	E = Al in Eq. (1)	E = Zn in Eq. (1)
f_v (%)	4.6	4.4	4.1

4. Conclusion

After ageing at 140 °C for 24 hours, the Al-Mg 5.55-Zn 1.35 alloy contains a large majority of hardening precipitates with the crystal structure and epitaxy relations that are characteristic of the T′ and T phases. These precipitates are regularly dispersed in the solute depleted solid solution. The morphology of the particles analysed by TAP has been visualized from 3D reconstruction. Elongated shapes of some precipitates have been evidenced.

The solute concentrations (at%) measured in the residual solid solution are 4.0 at% Mg and 0.3 at% Zn. This composition is fully coherent with the calculated volume fraction 4.5% and number density 1.8×10^{17} cm^{-3} of particles.

The compositions of the precipitates, as measured in their core part, present a relatively low scatter around the mean value 37.5 at% Mg, 36.5 at% Al and 26 at% Zn which is very close to the composition $Mg_{32}(Al, Zn)_{49}$ of the equilibrium T phase. However, the surface of particles was found to contain much less magnesium than the heart, whereas the zinc level remains high. This coring phenomenon reveals that the precipitates present in the alloy at this stage of ageing are probably not the equilibrium phase, which is an argument in favor of distinguishing the T′ phase from the T phase.

Acknowledgments

The authors would like to thank Pechiney Rhénalu for providing the alloy used in this study.

References

[1] Schmuck C., Auger P., Danoix F. and Blavette D., *Appl. Surf. Sci.* **87/88** (1995) 228-233.
[2] Bigot A., Danoix F., Auger P., Blavette D. and Reeves A., *Mater. Sci. Forum* **217-222** (1996) 695-700.
[3] Auld J.H. and Cousland S.Mck., *Metal Sci.* (December 1976) pp. 445-448.
[4] Bergman G., Waugh J.L.T. and Pauling L., *Acta Cryst.* **10** (1957) 254-258.
[5] Auld J.H. and Cousland S.Mck., *Journ. Australian Inst. Met.* **19** (1974) 194-199.
[6] Kaygodorova L.I., Komarova M.F., Buynov N.N., Belousov N.N. and Kashevnik L.YA., *Phys. Met. Metall.* **48** (1981) 66-75.
[7] Bernole M., Graf R., *Mem. Sci. Rev. Met.* **69** (1972) 123-133.
[8] Glanz J., *R&D Magazine* **34** (1992).
[9] Blavette D., Deconihout B., Bostel A., Sarrau J.M., Bouet M. and Menand A., *Rev. Sci. Instr.* **64** (1993) 2911-2919.
[10] Bas P., Bostel A., Grancher G., Deconihout B. and Blavette D., *Appl. Surf. Sci.* **94/95** (1996) 442.